Progress In Electromagnetics Research C, Vol. 24, 235–249, 2011

TRI-BAND FOUR-ELEMENT MIMO ANTENNA WITH HIGH ISOLATION

J.-F. Li*, Q.-X. Chu, and X.-X. Guo

School of Electronic and Information Engineering, South China University of Technology, Guangzhou 510640, China

Abstract—A tri-band four-element MIMO (multiple-input-multiple-output) antenna with high isolation is presented. The MIMO antenna consists of four symmetrical antenna elements. To relieve the degradation of the operation bandwidth caused by the strong mutual coupling among the four antenna elements, four symmetrical rectangles are removed from the four corners of the ground plane, respectively. The effect of the cutting of the four rectangles on the isolation is slight. Two kinds of isolation structure are applied to reduce the mutual coupling among the elements. The first kind of isolation consists of two slits and a protruded ground branch, and the second kind of isolation structure consists of four symmetrical slits etched into the ground plane. The mutual coupling caused by surface currents is reduced by slits, the mutual coupling resulted from near-field is suppressed by the ground branches, and thus high isolation for the MIMO antenna is achieved. Moreover, the effects of the slits and the ground branches on the operation bandwidth are slight, thus the operation bandwidth and the mutual coupling can be controlled independently, to some degree. A tri-band operation bandwidth (2.34–2.95 GHz, 3.38–3.75 GHz, and 4.4–6.7 GHz) with VSWR ≤ 2 and isolation ≥ 20 dB, is achieved. The results, including S-parameters, radiation patterns, mean effective gain (MEG), radiation efficiency and signal correlations, indicate that the proposed MIMO antenna can provide spatial or pattern diversity to increase data capacity of wireless communication systems.

1. INTRODUCTION

Demand for the increased data capacity of wireless communication systems drives the development of MIMO systems [1–3]. In order to

Received 23 August 2011, Accepted 10 October 2011, Scheduled 15 October 2011

* Corresponding author: Jian-Feng Li (li.jf01@mail.scut.edu.cn).

achieve the desired performance of a MIMO system, the reduction of mutual coupling among the closely-placed antenna elements is necessary. When the number of antenna elements is increased, the mutual coupling will become more complicated and difficult to be reduced [4, 5]. Moreover, multi-band or broadband is required for the multifunctional terminal devices, and this further increase the difficulty of reducing mutual coupling.

To reduce the mutual coupling, decoupling network [6], inductor coil [7], ground branches [8], electromagnetic band-gap (EBG) structure [9] and an inverted-Y shaped stub inserted on the ground plane [10] were applied. All of the aforementioned ways were only used to enhance the isolation for two-element MIMO antennas. A series of slits etched into the ground plane [11], antennas placed uniquely [12] and orthogonal arrangement of antennas [13], were introduced to reduce the mutual coupling for four-element MIMO antennas. However, the four-element MIMO antennas [11–13] were not suitable for multifunctional terminal devices such as mobile phones, due to their narrow operation bandwidths or their large sizes.

A tri-band four-element MIMO antenna with high isolation is presented in this paper. The smallest edge-to-edge separation of the four symmetrical elements is about $0.058\lambda_0$ at 2.5 GHz. To relieve the degradation of the operation bandwidth caused by the strong mutual coupling among the four antenna elements, four symmetrical rectangles are removed from the four corners of the ground plane, respectively. The effect of the cutting of the four rectangles on the isolation is slight. Two kinds of isolation structure are applied to enhance the isolation. The first kind of isolation consists of two slits and a protruded ground branch, and the second kind of isolation consists of four symmetrical slits etched into the ground plane. The mutual coupling caused by surface currents is reduced by the etching slits, the mutual coupling resulted from the near-field is suppressed by the protruded ground branches, and thus low mutual coupling across the tri-band operation bandwidth of the proposed antenna is achieved. Moreover, the effects of the slits and the protruded ground branches on the operation bandwidth are slight, thus the operation bandwidth and the mutual coupling can be controlled independently, to some degree. Determined by VSWR $\leq$ 2 and isolation $\geq$ 20 dB, a tri-band bandwidth (2.34–2.95 GHz, 3.4–3.75 GHz and 4.4–6.7 GHz) is achieved, which covers 2.4/5.2/5.8-GHz WLAN and 2.5/3.5/5.5-GHz WiMAX systems. The geometry and the operation mechanism of the proposed MIMO antenna are discussed in Sections 2 and 3 respectively. In Section 4, the radiation patterns, MEG, radiation efficiency and signal correlations are calculated to evaluate the diversity

performance of the MIMO antenna. Finally, a conclusion is given in Section 5. The simulated and measured are in a good agreement, thus the proposed antenna can provide spatial or pattern diversity to increase data capacity of wireless communication systems.

2. ANTENNA CONFIGURATION

The geometry of the proposed MIMO antenna is illustrated in Fig. 1(a). The antenna is printed on a FR4 substrate with dimensions $89.6 \times 45 \times 1.6\,\text{mm}^3$, relative permittivity 4.4 and loss tangent 0.02. The antenna consists of four symmetrical element antennas (element #1, #2, #3 and #4), and the smallest edge-to-edge separation of the elements is $d = 7\,\text{mm}$. based on the formula (1), $d = 7\,\text{mm}$ is about $0.058\lambda_0$ at 2.5 GHz.

$$\lambda_0 = \frac{c}{f} \tag{1}$$

where, c and f denote the speed of light in vacuum and the frequency, respectively. The ground plane is printed on the back side of the substrate, and four symmetrical rectangles are removed from the four corners of the ground plane, respectively. The length and the width of each rectangle are $m_l = 9\,\text{mm}$ and $m_w = 4\,\text{mm}$, respectively. The first

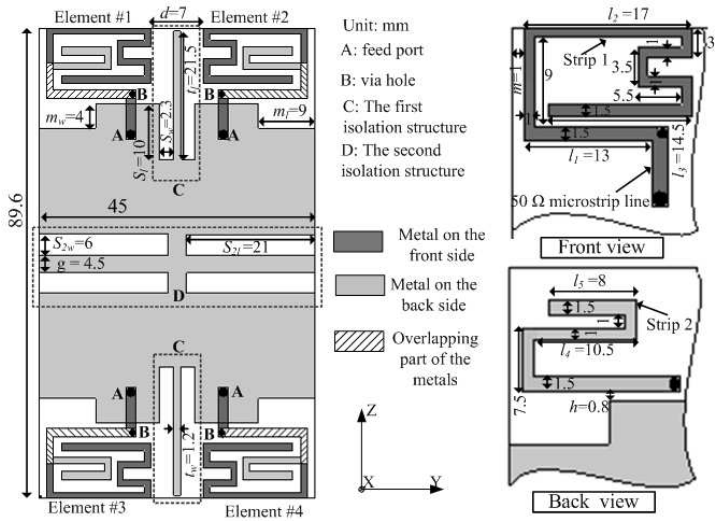

Figure 1. (a) structure of proposed MIMO antenna, (b) structure of element #1.

isolation structure consists of two slits ($S_l = 10\,\text{mm}$, $S_w = 2.3\,\text{mm}$) etched into the ground plane and a protruded ground branch ($t_l = 21.5\,\text{mm}$, $t_w = 1.2\,\text{mm}$). The second isolation structure is composed of four slits ($S_{2l} = 21\,\text{mm}$, $S_{2w} = 6\,\text{mm}$) etched into the middle of the ground plane, and the space between the two parallel slits is $g = 4.5\,\text{mm}$. In following, we only discuss element #1 because of the symmetric configuration. The detail dimensions of element #1 are shown in Fig. 1(b). Element #1 of size $17 \times 12.3 \times 1.6\,\text{mm}^2$ consists of two metal strips (strip 1 and strip 2). The strip 1 printed on the front side of the substrate is directly connected to a $50\,\Omega$-microstrip line, and the strip 2 connected to the $50\,\Omega$-microstrip line through a via hole is placed on the back side of the substrate. The lengths of strip 1 and 2 are chosen as 71 and 40 mm, respectively, the two-strip of size $13 \times 1.5 + 7.5 \times 1\,\text{mm}^2$ is the overlapping part of the two strips, and the space between the antenna element and the ground plane is $h = 0.8\,\text{mm}$.

3. DESIGN PROCESS AND OPERATION MECHANISM

The design process and the operation mechanism of the proposed MIMO antenna are analyzed in this section. Because of the symmetric configuration of the four antenna elements, only $|S_{11}|$, $|S_{21}|$, $|S_{31}|$ and $|S_{41}|$ are studied. $|S_{11}|$ denotes the reflection coefficient of element #1 and $|S_{21}|/|S_{31}/|S_{41}|$ presents the mutual coupling between element #1 and #2/#3/#4.

3.1. One-element Antenna

Investigation of the one-element antenna as shown in Fig. 2 can help to understand the operation mechanism of the proposed four-element MIMO antenna. In Fig. 2, the size of substrate is select to $59 \times 23 \times 1.6\,\text{mm}^3$, and l_1, l_2, l_3, l_4, l_5, m and h are chosen as 15.5, 20, 15.5, 14, 11, 2.5 and 2.5 mm, respectively, for achieving the best result. Based on the formula (2) [14, 15], the length of the strip 1 is 77 mm which is about 1.0λ at 2.4 GHz, and the length of strip 2 is 49 mm which is about 1.0λ at 3.0 GHz.

$$L = \frac{c}{Nf_r}\left(\sqrt{\frac{\varepsilon_r + 1}{2}}\right)^{-1} \tag{2}$$

where, L, N, f_r, and ε_r are the length of antenna, the number of resonant mode, the resonant frequency, and the relative permittivity of the substrate.

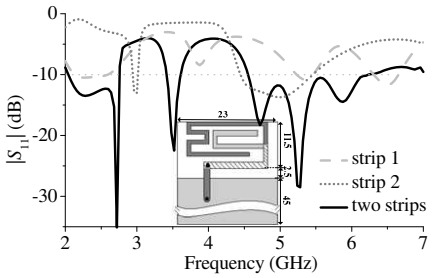

Figure 2. Structure and $|S_{11}|$ of a one-element antenna and $|S_{11}|$ of two cases with strip 1 only or strip 2 only.

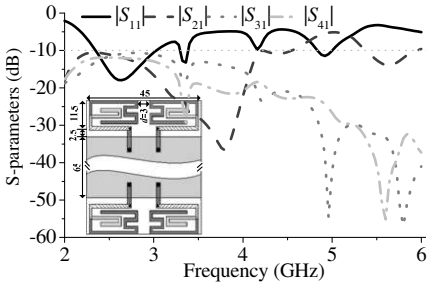

Figure 3. Structure and S-parameters of a MIMO antenna with a conventional ground plane.

The simulated $|S_{11}|$ of the one-element antenna and two cases with strip 1 only or strip 2 only are also shown in Fig. 2. According to the formula (2) and the results shown in Fig. 2, it can be concluded that the case only with strip 1 generates 1.0λ resonant mode at about 2.4 GHz, 1.5λ resonant mode at about 3.8 GHz and 2.0λ dual-resonance excitation at about 6.0 GHz, while the case only with strip 2 generates 1.0λ resonant mode at about 3.0 GHz and 1.5λ resonant mode at about 4.8 GHz. When the two strips are integrated together, the two-strip structure introduces additional capacitance to the inductive antenna to enhance the impedance matching, thus a wide tri-band is achieved. With $|S_{11}| \leq -10$ dB, the first, the second and the third band are 2.04–2.74 GHz, 3.4–3.6 GHz and 4.55–6.15 GHz, respectively.

3.2. Integration of Four Antenna Elements

The one-element antenna discussed in Part 3.1 is suitable to be an antenna element of a MIMO antenna for 2.4/5.2/5.8-GHz WLAN and 2.5/3.5/5.5-GHz WiMAX application. In Fig. 3, these four antennas with the smallest edge-to-edge separation of $d = 3$ mm are integrated on a FR4 substrate of size $93 \times 45 \times 1.6\,\text{mm}^3$, and the parameters of antenna elements are the same as the those shown in Fig. 2. Compared with the result given in Fig. 2, the integration of the four elements leads to poor operation bandwidth and poor isolation. That is because that the excited element induces strong currents distributing on the ground plane and the non-excited elements as shown in Fig. 4. In Fig. 4, element #1 is excited, while the other three elements are terminated with 50 Ω loads.

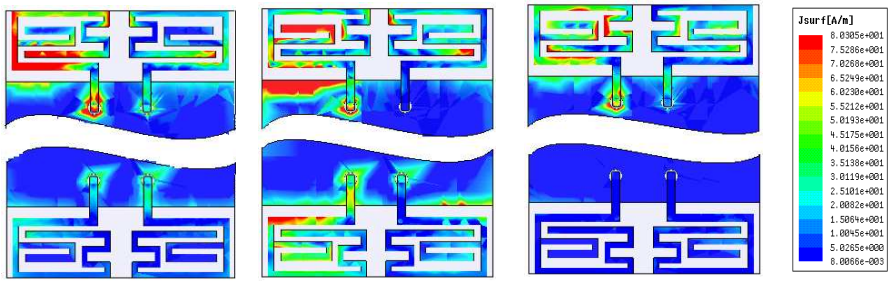

(a) (b) (c)

Figure 4. Current distributions of the four-element MIMO antenna with a conventional ground at (a) 2.5 GHz, (b) 3.5 GHz and (c) 5.5 GHz.

3.3. Improvement of Operation Bandwidth

In Fig. 5, four symmetrical rectangles of size $m_l \times m_w$ are removed from the four corners of the ground plane, respectively. To get the best result, l_1, l_2, l_3, l_4, l_5 and h are selected to 13, 17, 14.5, 9.5, 8 and 0.8 mm, respectively, while keeping other dimensions fixed. In Fig. 6, it can be observed that the cutting of the four rectangles from the ground plane can help to decrease the induced capacitance resulted from the integration of the four antennas on a FR4 substrate. That is to say, the cutting of the four rectangles from the ground plane can relieve the distortion of the impedance matching caused by the strong mutual coupling among the four antenna elements. The effects of m_l, m_w, and h on $|S_{11}|$ are shown in Fig. 7, and a good operation bandwidth is obtained when m_l, m_w, and h are select to 9, 5 and 0.8 mm respectively. With $|S_{11}| \leq -10$ dB, the first, the second and the third impedance band are 2.38–3.2 GHz, 3.4–3.6 GHz and 4.38–6.3 GHz, respectively. From Figs. 3 and 5, it is observed that the effect of the cutting of the four rectangles on the mutual coupling is slight. Therefore, it is necessary to find a way to reduce the strong mutual coupling.

3.4. Enhancement of $|S_{21}|$

The strong mutual coupling among the antennas closely spaced is caused by the ground surface current and the near-field. Etching slits into the ground plane is an effective way to reduce the mutual results form the ground surface current [16, 17], and a reflector can decrease the mutual coupling caused by the near-field through separating the radiation patterns of the antennas [18]. Therefore, it is to try to

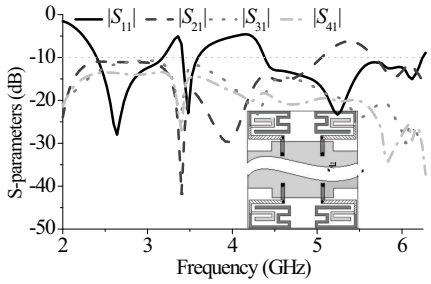

Figure 5. Structure and S-parameters of the four-element antenna with four removing rectangles.

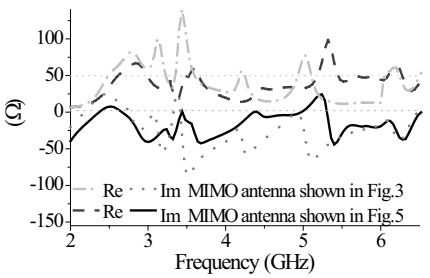

Figure 6. Comparison of the input impedance.

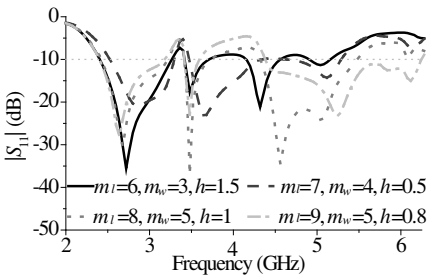

Figure 7. $|S_{11}|$ of the MIMO antenna shown in Fig. 5 with different m_l, m_w and h.

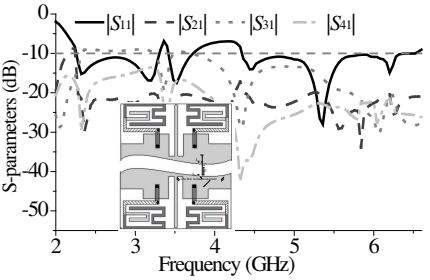

Figure 8. Structure and S-parameters of the antenna with the first isolation structure.

integrate the two ways to reduce the mutual coupling between element #1 (#3) and element #2 (#4) in this paper, and the first kind of isolation structure is introduced as shown in Fig. 8. This kind of isolation structure consists of two slits of size $S_l \times S_w$ and a ground branch of size $t_l \times t_w$. The dimensions of the MIMO antenna are the same as those shown in Fig. 7 except for m and h, and m and h are both changed to 1 mm.

The current distributions of the MIMO antenna with element #1 excited and the other elements terminated with 50 Ω loads at 2.5, 3.5 and 5.5 GHz are exhibited in Fig. 9, which can help to reveal the operation mechanism of the isolation structure. In Fig. 9, a large portion of the induced ground surface currents which are caused by the element #1, is being trapped by the slits. It demonstrates that currents flowing from left-hand side of the ground plane to right-hand side are

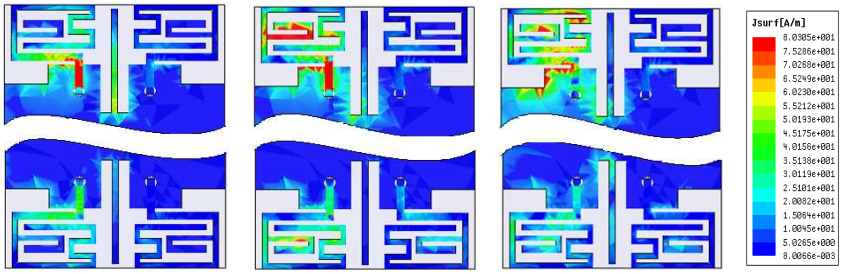

Figure 9. Current distributions of the four-element MIMO antenna with the first isolation structure at (a) 2.5 GHz, (b) 3.5 GHz and (c) 5.5 GHz.

substantially reduced, and the induced currents observed on element #2 are smaller as compared to Fig. 4. Therefore, the mutual coupling between element #1 and #2 caused by the ground surface currents is reduced. The protruded ground branch can decrease the mutual coupling caused by the near-field through separating radiation patterns of element #1 and #2, and the radiation patterns of the MIMO antenna will be analyzed in detail in Section 4. It can be concluded that this kind of isolation structure can reduce the mutual coupling caused by the surface currents, and the near-field, and therefore low mutual coupling between element #1 and #2 is achieved despite that the edge-to-edge separation of the two elements is only 7 mm.

The application of the first kind of isolation structure provides -9, -2 and -14 dB improvement of $|S_{21}|$ for the first, the second and the third band, respectively, over the MIMO antenna shown in Fig. 5, and it also provides -3 dB improvement of $|S_{41}|$ for the third band. The simulated $|S_{21}|$ as a function of varying S_w, S_l, t_w and t_l is shown in Fig. 10. When S_w, S_l, t_w and t_l are chosen as 2.3, 10, 1.2 and 21.5 mm, respectively, $|S_{21}|$ is lower than -20 dB within the three operation bands. From Figs. 5 and 8, it can be observed that the effects of the first isolation structure on $|S_{11}|$ and $|S_{31}|$ are slight.

3.5. Enhancement of $|S_{31}|$

The distance between the element #1 (#2) and #3 (#4) is large, the mutual coupling between the two elements is mainly caused by the ground surface current which can be reduced by etching slits into the ground plane effectively. Therefore, the second isolation structure is introduced as shown in Fig. 1. The dimensions of the MIMO antennas

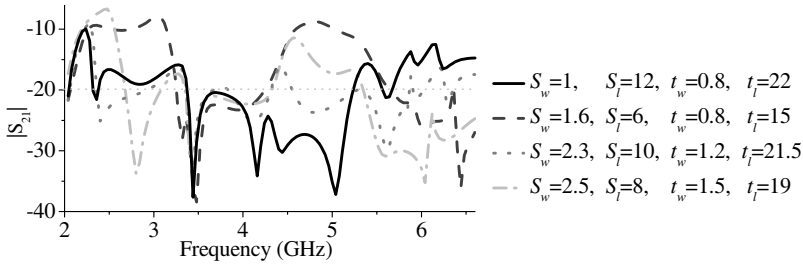

Figure 10. $|S_{21}|$ of the MIMO Antenna with the first isolation structure with varying s_w, s_l, t_w and t_l.

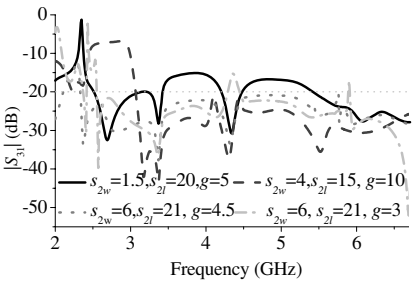

Figure 11. $|S_{31}|$ of the proposed MIMO antennas shown in Fig. 1 with varying s_{2w}, s_{2l}, and g.

Figure 12. Photographs of the fabricated antenna: (a) front view, (b) back view.

shown in Figs. 1 and 8 are the same except for h which is chosen as 0.8 mm in Fig. 1. The variations of S_{2l}, S_{2w} and g have great influence on $|S_{31}|$ as shown in Fig. 11. When S_{2l}, S_{2w} and g are chosen as 21, 6, and 4.5 mm, respectively, $|S_{31}|$ is smaller than -20 dB across the three operation bands.

The proposed MIMO antenna has been fabricated and tested, and the photos of the fabricated MIMO antenna are shown in Fig. 12. The simulated and measured S-parameters are in a good agreement as observed in Fig. 13. Discrepancy of $|S_{11}|/|S_{21}|$ between the results shown in Figs. 8 and 13 is small. From Figs. 8 and 13, it can be observed that the application of the second isolation structure provides -14, -13 and -7 dB improvements of $|S_{31}|$ for the first, the second and the third band, respectively. Moreover, it also provides -6,

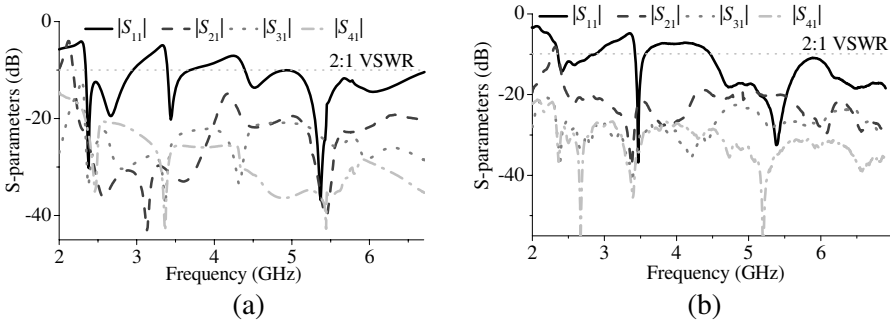

Figure 13. S-parameters of the proposed MIMO antenna (a) simulated results, (b) measured results.

-10 and -6 dB improvements of $|S_{41}|$ for the first, the second and the third operation band, respectively. Determined by VSWR ≤ 2 and isolation ≥ 20 dB, the first operation bandwidth is 2.34–2.95 GHz covering the following bands: 2.4-GHz WLAN (2.4–2.48 GHz) and 2.5-GHz WiMAX (2.5–2.69 GHz); the second operation bandwidth is 3.38–3.75 GHz covering 3.5-GHz WLAN (3.4–3.6 GHz); the third operation bandwidth is 4.4–6.7 GHz which fulfills the required bandwidths of 5.2-GHz WLAN (5.15–5.35 GHz), 5.5-GHz WiMAX (5.25–5.85 GHz) and 5.8-GHz WLAN (5.725–5.825 GHz) systems.

4. DIVERSITY PERFORMANCE OF THE PROPOSED MIMO ANTENNA

The proposed MIMO antenna exhibits the high isolation property, to some degree, also due to the special radiation patterns. The simulated and measured 2-D radiation patterns of the MIMO antenna (element #1 is excited and the other elements are terminated with 50 Ω loads) at 2.5/3.5/5.5 GHz are shown in Fig. 14, and the measured and simulated results are in a good agreement. For the element #1, the protruded ground branch is viewed as a reflector, which can reflect a portion of energy radiated by element #1 along the $+y$-axis. Therefore, the maximum gain of element #1 is not along the $+y$-axis where element #2 is located at the corner of the ground plane. The main ground also can be seen as a reflector for the element #1, and a part of energy radiated by element #1 is reflected by the main ground plane. Consequently, the maximum gain of element #1 is also not along the $-z$-axis where element #3 is located at the corner of the ground plane. Element #2, being a mirror image of element #1

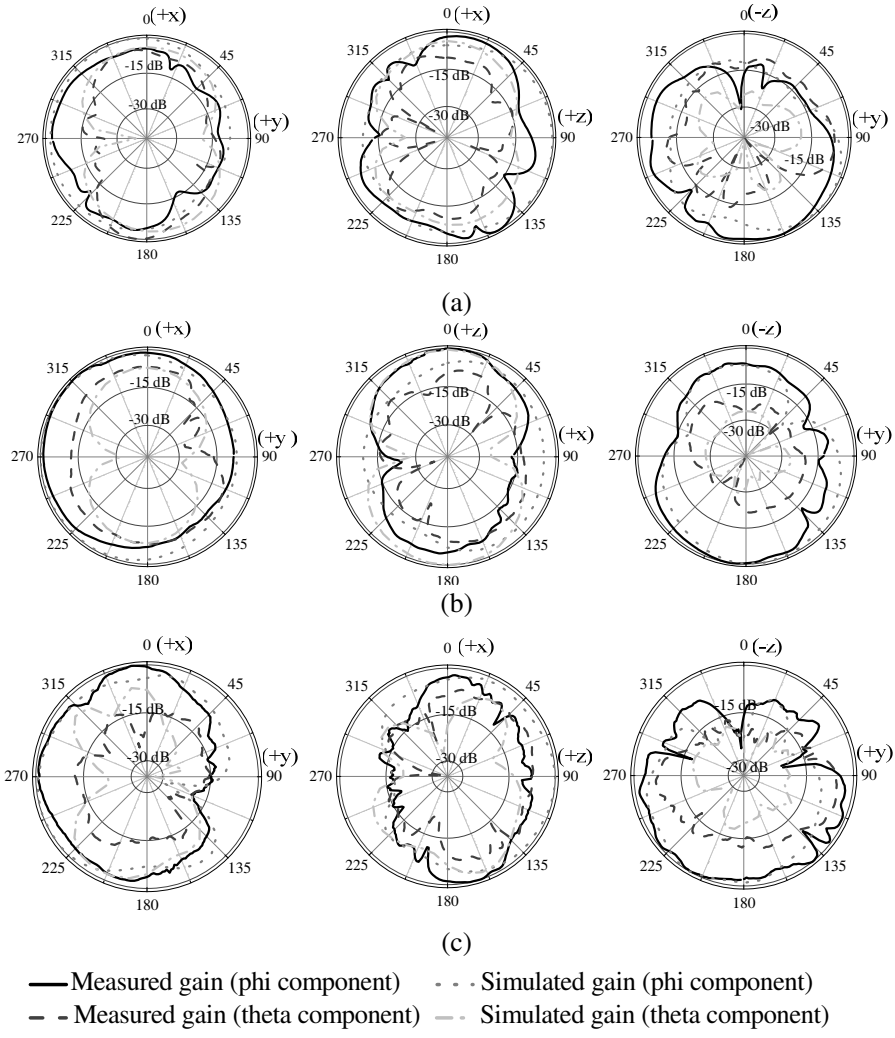

Figure 14. Simulated and measured gain patterns at (a) 2.5 GHz, (b) 3.5 GHz and (c) 5.5 GHz.

along the x-z plane, does not have maximum gain along the $-y$-axis and $-z$-axis, where element #1 and #4 are located at the two corners, respectively. Element #3, being a mirror image of element #1 along the x-y plane, does not have maximum gain along the $+y$-axis and $+z$-axis, where element #4 and #1 are located at the two corners, respectively. Element #4, being a mirror image of element #3 along the x-z plane, does not have maximum gain toward the $-y$-axis and $+z$-axis, where element #3 and #1 are located at the

two corners, respectively. The maximum gains of the four elements are in different four directions, back-radiation patterns for the four elements are observed, which means the particular radiation patterns are complementary to each other, and therefore, the proposed MIMO antenna can receive or transmit the signal in all direction to realize the spatial diversity. Moreover, this particular radiation patterns can help to reduce mutual coupling induced by the near-field.

MEGs are calculated based on a series of the assumption of mobile wireless environments defined in [19]. In this paper, a cross-polarization discrimination Γ of 0 dB, which is the average in an indoor fading environment [19, 20], is assumed, and the calculated MEGs based on the measured data at 2.5, 3.5 and 5.5 GHz are shown in Table 1. The calculated radiation efficiencies η are also listed in Table 1. The maximum ratio of the MEGs is smaller than 0.1 dB, and η are larger than 75%.

Finding in [21], the envelope correlation ρ and envelope correlation coefficient ρ_e between antennas i and j in an N-element MIMO antenna system can be calculated:

$$|\rho(i,j,N)|^2 = \rho_e(i,j,N) = \left| \frac{\sum_{n=1}^{N} S_{i,n}^* S_{n,j}}{|\Pi_{k=i,j} \left(1 - \sum_{n=1}^{N} S_{k,n}^* S_{n,k}\right) \cdot \Pi_{n=1}^{N} \eta_n|^{1/2}} \right|^2 \tag{3}$$

where, i, j = 1, 2, 3, 4, and N = 4. Based on the measured data, ρ at the central frequencies of the three operation bands of the proposed MIMO antenna are calculated, and the results are shown in Table 2. From Table 2, it can be seen that ρ is smaller than 0.1.

Table 1. Performance of the prototype of the proposed antenna.

f (GHz)	MEG_1 (dB)	MEG_2 (dB)	MEG_3 (dB)	MEG_4 (dB)	η_1 (%)	η_2 (%)	η_3 (%)	η_4 (%)
2.5	−4.50	−4.15	−4.86	−4.29	81.0	80.2	81.8	82.3
3.5	−6.17	−6.59	−6.02	−6.85	75.5	76.8	77.3	75.8
5.5	−4.35	−4.53	−4.56	−4.29	83.4	84.5	85.2	83.1

Table 2. Performance of the prototype of the proposed antenna.

f (GHz)	$\rho_{12} \approx \rho_{21} \approx \rho_{34} \approx \rho_{43}$	$\rho_{13} \approx \rho_{31} \approx \rho_{24} \approx \rho_{42}$	$\rho_{14} \approx \rho_{41} \approx \rho_{23} \approx \rho_{32}$
2.5	0.086	0.054	0.034
3.5	0.044	0.026	0.019
5.5	0.027	0.020	0.018

5. CONCLUSION

A tri-band four-element MIMO antenna with high isolation has been presented. The cutting of four rectangles from the four corners of the ground plane, respectively, has been used to improve the operation bandwidth, and two kinds of isolation structures have been introduced to enhance the isolation of the four antenna elements. The operation mechanisms of the proposed MIMO antenna have been discussed. To some degree, the impedance bandwidth and the mutual coupling can be controlled independently. Determined by VSWR ≤ 2 and isolation $\geq$ 20 dB, a tri-band bandwidth (2.34–2.95 GHz, 3.38–3.75 GHz and 4.4–6.7 GHz) was achieved. Back-radiation patterns for the four elements were achieved, and the MEGs, radiation efficiency, and correlation coefficients have been calculated. All results indicated that the proposed antenna can provide spatial or pattern diversity to increase data capacity of wireless communication systems.

ACKNOWLEDGMENT

This work is supported by the Science Fund of China (60971052), and the Fundamental Research Funds for the Central Universities (2009IM0167).

REFERENCES

1. Karaboikis, M. P. and V. C. Papamichael, "Integrating compact printed antennas onto small diversity/MIMO terminals," *IEEE Trans. Antennas Propag.*, Vol. 56, No. 7, 2067–2078, Jul. 2008.
2. Wen, G., "Multi-antenna information theory," *Progress In Electromagnetics Research*, Vol. 75, 11–50, 2007.
3. Mallahzadeh, A. R., H. Oraizi, and Z. Davoodi-Rad, "Application of the invasive weed optimization technique for antenna configurations," *Progress In Electromagnetics Research*, Vol. 79, 137–150, 2008.
4. Abouda, A. A. and S. G. Haggman, "Effect of mutual coupling capacity of MIMO wireless channels in high SNR scenario," *Progress In Electromagnetics Research*, Vol. 65, 27–40, 2006.
5. Keowsawat, P., C. Phongcharoenpanich, S. Kosulvit, J.-I. Takada, and M. Krairiksh, "Mutual information of MIMO system in a corridor environment based on double directional channel measurement," *Journal of Electromagnetic Waves and Applications*, Vol. 23, No. 8–9, 1221–1233, Jun. 2009.

6. Chen, S. C., Y. S. Wang, and S. J. Chung, "A decoupling technique for increasing the port isolation between two strongly coupled antennas," *IEEE Trans. Antennas Propag.*, Vol. 56, No. 12, 3650–3658, Dec. 2008.
7. Krairiksh, M., P. Keowsawat, C. Phongcharoenpanich, and S. Kosulvit, "Two-probe excited circular ring antenna for MIMO application," *Progress In Electromagnetics Research*, Vol. 97, 417–431, 2009.
8. Zhu, F. G., J. D. Xu, and Q. Xu, "Reduction of mutual coupling between closely-packed antenna elements using defected ground structure," *Electronics Lett.*, Vol. 45, No. 12, Jun. 2009.
9. Payandehjoo, K. and R. Abhari, "Employing EBG structures in multiantenna systems for improving isolation and diversity gain," *IEEE Antennas and Wireless Propag. Lett.*, Vol. 8, 1162–1165, 2009.
10. Najam, A. I., Y. Duroc, and S. Tedjni, "UWB-MIMO antenna with novel stub structure," *Progress In Electromagnetics Research C*, Vol. 19, 245–257, 2011.
11. Xiong, H., J. Li, and S. He, "A compact planar MIMO antenna system of four elements with similar radiation characteristics and isolation structure," *IEEE Antennas and Wireless Propag. Lett.*, Vol. 8, 1107–1110, 2009.
12. Fakhr, R. S., A. A. Lotfi Neyestanak, and M. Naser-Moghadasi, "Compact size and dual band semicircle shaped antenna for MIMO application," *Progress In Electromagnetics Research C*, Vol. 11, 147–154, 2009.
13. Mallahzadeh, A. R., S. Es'haghi, and A. Alipour, "Design of an E-shape MIMO antenna using IWO algorithm for wireless application at 5.8 GHz," *Progress In Electromagnetics Research*, Vol. 90, 187–203, 2009.
14. Diallo, A., C. Luxey, and P. L. Thuc, "Study and reduction of the mutual coupling between two mobile phone PIFAs operating in the DCS 1800 and UMTS bands," *IEEE Trans. Antennas Propag.*, Vol. 54, No. 11, 3063–3074, 2006.
15. Deepti, D. K., M. Gopikrishna, and C. K. Anand, "CPW-fed koch fractal slot antenna for WLAN/WiMAX applications," *IEEE Antennas and Wireless Propag. Lett.*, Vol. 7, 389–392, 2008.
16. Chiu, C. Y., C. H. Cheng, and R. D. Murch, "Reduction of mutual coupling between closely-packed antenna elements," *IEEE Trans. Antennas Propag.*, Vol. 55, No. 6, 1732–1738, Jun. 2007.

17. Zhu, F. G., J. D. Xu, and Q. Xu, "Reduction of mutual coupling between closely-packed antenna elements using defected ground structure," *Electronics Lett.*, Vol. 45, No. 12, Jun. 2009.
18. Chi, G. M., B. H. Li, and D. S. Qi, "Dual-band printed diversity antenna for 2.4/5.2-GHz WLAN application," *Microw. Opt. Tech. Letts.*, Vol. 45, No. 6, 561–563, Jun. 2005.
19. Ko., S. C. K. and R. D. Murch, "Compact integrated diversity antenna for wireless communications," *IEEE Trans. Antennas Propag.*, Vol. 49, 954–960, Jun. 2001.
20. Ding, Y., Z. Du, K. Gong, and Z. Feng, "A novel dual-band printed diversity antenna for mobile terminals," *IEEE Trans. Antennas Propag.*, Vol. 55, No. 7, 2088–2096, Jul. 2007.
21. Thaysen, J. and K. Jakobsen, "Envelope correlation in (N, N) MIMO antenna array from scattering parameters," *Microw. Opt. Tech. Letts.*, Vol. 48, No. 5, 832–834, May 2006.